

N90-21336

SHORT WAVELENGTH HgCdTe STARING FOCAL PLANE FOR LOW BACKGROUND ASTRONOMY APPLICATIONS*

8 February 1989

J. Stobie, N. Hartle, D. Lacroix, K. Maschhoff
Honeywell Electro-Optics Division
Lexington Massachusetts 02173

ABSTRACT

The design of a 128x128 staring SWIR HgCdTe focal plane incorporating charge integrating transimpedance input preamplifiers is presented. The preamplifiers improve device linearity and uniformity, and provide signal gain ahead of the multiplexer and readout circuitry. Detectors with cutoff wavelength of 2.5 microns and operated at 80 K have demonstrated impedances in excess of 10^{16} ohms with 60 percent quantum efficiency. Focal plane performance using a smaller format device is presented which demonstrates the potential of this approach. Although the design is capable of achieving less than 30 rms electrons with today's technology, initial small format devices demonstrated a read noise of 100 rms electrons and were limited by the atypical high noise performance of the silicon process run. Luminescence from the active silicon circuitry in the multiplexer limits the minimum detector current to a few hundred electrons per second. Approaches to eliminate this excessive source of current is presented which should allow the focal plane to achieve detector background limited performance.

1.0 INTRODUCTION

Infrared astronomy is yielding significant quantities of data to enhance our understanding of the universe. However, unlike the visible spectrum the infrared sensor technology has not matured as rapidly. Sensors which dramatically reduce the exposure time of a two dimensional observation to 1 to 1000 seconds, while achieving zodiacal background limited performance in the short wavelength 1 to 2.5 micron range would significantly advance this branch of astronomy. This implies a large staring sensor format with small diffraction limited elements. The sensor's noise must be less than the shot noise of the collected signal and the detectors dark current, for space based observations, less than the zodiacal background of 10 photons per second near 1.4 microns. The focal plane should be capable of multiple nondestructive reads to support off focal plane signal processing to optimize the sensors sensitivity and to provide immunity to spurious noise, such as events caused by gamma radiation. Additional system requirements emphasize good linearity and system stability for accurate radiometric measurements with minimal system calibration and maintenance.

Short wavelength, 1 to 3 micron, HgCdTe photovoltaic detectors have demonstrated RoA products of 10^{12} ohms-cm² at temperatures below 100 K.[1,2] Thus at 80 K the detector's thermal noise should be below the zodiacal background noise. This noise performance coupled with high quantum efficiency, better than 70 percent, provides ample sensitivity. Furthermore imaging requirements can be satisfied using current processing technology to fabricate small 2 mil detectors arranged in a staring format exceeding 100 elements on a side.

The small detector size also yields a device with small capacitance, less than 250 femtofarads, which is beneficial for a low noise coupling scheme. Ideally, the detector

should be operated at or near zero bias to minimize any nonlinear effects introduced by the detector's capacitance-voltage characteristics and to minimize dark current and detector $1/f$ noise. These requirements lead to an input circuit design using a charge integrating transimpedance differential amplifier. Negative feedback maintains a constant detector bias which is adjustable by the voltage placed on the non-inverting input terminal. Honeywell has completed the design of a SWIR 128 x128 staring multiplexer incorporating this input preamplifier in each unit cell. This preamplifier is designed to boost the signal voltage by a factor of 10 in order to minimize the effects of subsequent signal processing functions, such as the multiplexing and off focal plane data acquisition system, on the signal integrity. This latest design benefits from its predecessor, a small format multiplexer^[4], developed specifically to demonstrate the merits of the charge integrating differential preamplifier approach.

The performance of the small format hybrid focal plane is summarized in Table I along with the performance expected for the 128x128 focal plane. The measured performance of this small format device compares very well with the theory and the parameters measured for the detector array and multiplexer. This direct conformation of the performance model has given us the confidence to conservatively predict the performance for the 128x128 SWIR focal plane.

A description of the 128x128 focal plane is given in the following section. The next three sections will discuss the performance obtained with the small format focal plane; Section 3 will present the detector performance, Section 4 will discuss the multiplexer, and Section 5 addresses the focal plane performance. Finally section 6 will address approaches adopted to further improve the performance of the 128 x 128 staring focal plane.

2.0 Description of the 128 X128 Focal plane

The 128 x128 focal plane is a hybrid focal plane consisting of a photovoltaic HgCdTe detector array on 2 mil centers bump mounted to a silicon CMOS readout multiplexer. A block diagram of the device is shown in Figure 1. The central 128 x128 detector imaging core is embedded within a 132 x132 hybrid array to greatly reduce edge effects. The multiplexer actually contains a matrix of 136 x136 cells where the outermost input cells do not have corresponding detector elements and are included to monitor the multiplexer performance independent of the detectors. The benefits of these additional cells far outweigh the 13 percent increase in the total readout time.

The backside illuminated detectors are fabricated on LPE grown HgCdTe material on a CdTe substrate. The planar design uses a ground ring around each element to improve detector definition as shown in Figure 2. The design yields a fill factor of 80 percent with an expected crosstalk of 3 percent. The fabrication of these arrays uses standard processing techniques. Based on measurements of 4 mil square detectors the detector resistance should exceed 10^{16} ohms at 80 K and have a backside illuminated quantum efficiency of 70 percent with an AR coating on the CdTe substrate. The detector capacitance, even at zero bias, is expected to be less than 200 femtofarads.

The readout multiplexer uses proven low power X-Y addressable analog multiplexers and proven transimpedance input preamplifiers to achieve a read noise capability of 30 rms electrons. The multiplexer configuration is shown in Figure 3. Each detector element is connected to an input preamplifier which integrates and converts this signal to a voltage. An array of analog switches composed of row and column select switches are addressed to sequentially connect each input to the output buffer. Two low-power CMOS digital shift

registers, located along the periphery of the chip, generate the address pulses for the analog switches.

Each input preamplifier is a charge-integrating high gain differential amplifier as shown in Figure 4. A well-defined feedback capacitor is used to integrate the detector current and maintain constant bias across the detector to insure good linearity. The common V_{bias} line connected to every amplifier is used to maintain near zero bias (3 mv, 1 sigma, about a nominal -10 mv) operation across the entire detector array for uniform gain and to minimize dark current and detector 1/f noise. The reset switch across the feedback capacitor is used to initialize the circuit prior to each integration cycle. Signal gain is obtained by using a feedback capacitance which is less than the detector's capacitance. The design uses a signal gain of order 10 to minimize the effect of any additional noise contribution of the readout circuitry. The charge capacity is 1.6×10^5 electrons.

As a goal the response linearity of the focal plane should be better than 1 percent and is dependent upon the current response characteristics of the photodiode, the charge to voltage linearity of the integrating capacitors, and the voltage linearity of the subsequent buffers ahead of the digitizer. The current response of photodiodes is well documented and shown to be linear over several orders of magnitude, and properly designed voltage followers are also linear to better than 1 percent. The characteristics of the integrating capacitor can be a major contributor to nonlinear response. This is particularly true for direct readout devices which rely on the detectors own capacitance. A typical capacitance versus voltage plot of a SWIR HgCdTe detector at 80 K is shown in Figure 5. For most reasonable ranges of integrated input signal the nonlinearity introduced by the detector's own capacitance remains outside the 1 percent maximum. Postprocessing functions are required to store gain and offset normalization curves for each detector as a function of initial and final voltages during an exposure. Establishment and maintenance of these calibration look-up tables is a important requirement for the system.

A major advantage of the high gain integrating input circuit is its removal of this source of nonlinearity by integrating the detector current across a stable feedback capacitor. This capacitor exhibits very stable charge-voltage characteristics to yield a linear response better than 1 percent over the full range in detector currents. Present photo-lithographic tolerances will maintain a variation in capacitance below 5 percent. Furthermore, the virtues of negative feedback allows the multiplexer to maintain a virtually constant detector voltage (less than 0.5 mv change) across the detector diode, which leads to a significant reduction in detector dark current nonuniformity.

The ultra-low read noise performance of this hybrid FPA is made possible by a design which readily supports multiple non-destructive read cycles, and through the use of simple postprocessing techniques. With a nominal 50 kilopixels/second readout rate the entire array can be readout every 370 milliseconds. Thus the reset level, the initial value at the start of the exposure as well as samples all along the integration cycle can be available for signal processing. Simple correlated sampling techniques are useful to eliminate the reset noise from the signal and bound the input 1/f noise. For long integration times the reset level is used to remove the uncertainties in the measurement due to electronic drift introduced by the buffers on the focal plane as well as in the data acquisition electronics.

The entire multiplexer chip dimension is 350 mils on a side as shown in Figure 6. A standard production 1.2 micron CMOS process allows this advanced input preamplifier to be contained within a 2 mil unit cell. Only three bias supplies and four clocks are required to operate the multiplexer. Under continuous readout operation the entire multiplexer will dissipate only about 80 milliwatts of power.

The present design of the 128 x 128 staring focal plane represents only a small

evolutionary step, clearly within the bound of today's technology, from its predecessor, a small 8 x 8 format feasibility focal plane. This small format device employed detectors on 4 mil centers using a readily available design and a custom built readout multiplexer to demonstrate the potential of this design approach. Even though the detectors in the 128 x 128 design are smaller, their expected performance parameters, including collection current, and impedances, have been conservatively determined by measurements obtained on the 4 mil detectors. The multiplexer performance, however, should be quite similar to those obtained on the small format multiplexer. This correlation is because the 8x8 multiplexer was specifically designed to demonstrate the actual performance potential of small 2 mil square unit cells with only a larger feedback capacitor to accommodate the larger detector current. Excellent overall focal plane performance for the large format design is determined by scaling the multiplexer performance with the electrical parameters of the 2 mil detector. The performance measurements of the small format device is presented below.

3.0 DETECTOR ARRAY PERFORMANCE

Excellent detector array performance has been obtained on both Honeywell bulk^[3] and LPE grown HgCdTe SWIR material. Since LPE offered shorter material lead times and the potential for better uniformity it has become our primary approach on this effort.

Detector array impedance measurements at high and moderate temperature (300 - 120K) were performed at Honeywell as a screening test using a ultra low-noise preamplifier with a feedback capacitor to eliminate the Johnson noise typically associated with a feedback resistor. Impedances are typically 10^8 ohms at 200 K and greater than 10^9 ohms at 175 K, following the expected theoretical temperature dependence for generation-recombination limited material as shown in Figure 7. As expected, at the nominal operating temperature of 80 K the detector impedance far exceeds the test capability of standard lab bench test equipment. In fact, the detector impedance can only be evaluated when hybridized to a low capacitance preamplifier similar to those incorporated in the multiplexer. The charge integrating differential amplifier used in the input cell provides a unique capability to directly measure the diode current-voltage characteristics. Typical diode characteristics measured at 80 K are shown in Figure 8 and array impedance uniformity is shown in Figure 9. Except for 3 elements all the detectors are between 0.4 and 4.0×10^{16} ohms. Scaling these results to 2 mil square detectors predicts impedances ranging from 0.7 to 11.0×10^{16} ohms with a corresponding thermal noise well below the zodiacal background shot noise.

High detector quantum efficiencies of 70 percent have been achieved over the 1.6 to 2.45 micron interval as shown in Figure 10. Below 1.4 microns the quantum efficiency may fall off quite dramatically, although there has been a considerable variation between the arrays measured as shown in the figure. The cause of this lower quantum efficiency at shorter wavelengths is still being considered with high back surface recombination velocity being a prime suspect. The data shown in Figure 10 is typical of non-AR coated detectors. An improvement as much as 20 percent can be anticipated with optimal AR coated detectors.

Analysis has shown that the detector capacitance linearly effects the total multiplexer read noise. Hence, capacitance below 250 femtofarads is required to achieve a low read noise for the 128 x 128 focal plane. Measurement of the 4 mil square feasibility detectors has shown a capacitance ranging from 400 to 600 femtofarads as shown in Figure 9. The device capacitance is principally the depletion layer capacitance which scales with the junction area. With the smaller 2 mil square detector a predicted capacitance of less than 180 femtofarads will be obtained.

Detector crosstalk well below 1 percent has been demonstrated on 4 mil square

detectors with a 77 percent fill factor. Since the fill factor and the crosstalk of these planar detectors are both controlled by the implant area and diffusion length, a tradeoff analysis was performed to determine the optimum implant configuration for the 2 mil detectors of the 128 x 128 array. A analysis predicts fill factor of 80 percent with a 3 percent crosstalk for the large format device.

4.0 MULTIPLEXER

Two process runs of small format multiplexers have been successfully completed. A layout oversight in the first run omitted bump vias for the detector common and rendered the multiplexers unusable for hybridization to detectors, but were still valuable in evaluating the performance of the multiplexer. The second run of multiplexers corrected this oversight and were integrated successfully with detectors.

Excellent multiplexer performance has been achieved and reported elsewhere^[4], so only the significant results which are pertinent to the performance of the hybrid focal plane will be discussed here. The multiplexer has proven to yield very low dark current, less than 2 electrons per second, low detector input offset variation with a peak to peak variation of less than 15 mv, and gain uniformity less than 1 percent. Linearity has been measured to within 2 percent for a nominal 1.0 volt full scale output swing. For the feasibility multiplexer the charge capacity of 3×10^5 electrons. Because smaller detectors will be used in the 128 x 128 focal plane the charge capacity has been reduced to 1.6×10^5 electrons.

The dominate source of read noise in the focal plane is due to the $1/f$ noise of the differential input amplifier. This source of noise is minimized by design, such as large p channel drive transistors, and effected by process related parameters such as interface trap density. The first lot of multiplexers exhibited typical values for input referred $1/f$ noise, $e_{1/f}(1 \text{ Hz})$ less than $1 \text{ uv}/\sqrt{\text{Hz}}$ at 1 Hz, as shown in Figure 11. Unfortunately the second multiplexer lot exhibited, as a result of process variation, an atypical high $1/f$ noise of about $6 \text{ uv}/\sqrt{\text{Hz}}$ which has severely limited the performance of the hybridized device.

With correlated double sampling the input $1/f$ noise contribution to the total rms noise of the focal plane is approximately given by:

$$\text{Noise}_{\text{rms}} = 2.13 \cdot (C_i + C_f) / q \cdot e_{1/f}(1 \text{ Hz}) \cdot (1 + \log(t_i \cdot f_{\text{CO}}))^{1/2} \quad (\text{rms electrons})$$

where C_i is the total input capacitance including the detector and any strays, C_f is the feedback capacitance, t_i is the integration time, and f_{CO} is the cutoff frequency. The logarithmic term accounts for the additional noise power contributed by the $1/f$ noise in each decade of frequency above the correlation frequency ($=1/t_i$). Thus for a reasonable multiplexed data rate of 50 kilopixels/second, the last factor in the equation amounts to less than 3. For the feasibility focal plane with a total input plus feedback capacitance is 0.6 pf the predicted input referred read noise is about 20 rms electrons, if the first lot of multiplexers had been used. Actual measurement using the second lot of multiplexer exhibit typical read noise of about 100 to 125 rms electrons, reflecting the significant impact the processing quality has on the focal plane performance.

The reset operation of the input integrating capacitor is not ideal and produces a voltage variation from reset to reset, known as reset noise. In addition the circuit requires a short time following the reset interval before equilibrium is attained. Typical relaxation

time is between 0.1 and 1 second as shown in Figure 12. The total settling response corresponds to a total input referred charge of about 2000 electrons which also varies from reset to reset. Two potential mechanisms for this relaxation time have been identified; circuit settling to pickup from the reset clock, or the relaxation of slow traps initially filled during the reset operation and integrated on the feedback capacitor. Relaxation time measurements which vary for different operating temperatures, could be used to identify the validity of the trap assisted mechanism.

Fortunately, simple correlated sampling techniques which take advantage of the multiple non-destructive readout capability of the multiplexer can be readily used to eliminate this offset variation (noise). In its simplest form two samples can be differenced, one taken at the beginning of an exposure and the other at the end of the integration cycle to remove the common reset offset and leave the integrated detector signal. Allowing for the circuit's settling time (0.1 to 1 second) before acquiring the initial sample will ensure the input has relaxed to equilibrium.

5.0 FOCAL PLANE PERFORMANCE

Performance measurements of the small format SWIR focal plane are in excellent agreement with the theory and performance parameters obtained from both the detector array and multiplexer. Scaling this performance to the 128x128 focal plane indicates that the SWIR focal plane requirements for space astronomy can be satisfied. The only disturbing measurements of the small format device was the presence of a relatively large detector current observable even under 100 percent cold shielding. This excessive current, which ranged from 100 to as high as 500 electrons per second, has been identified to be caused by luminescence photons emanating from the silicon multiplexer and which were not adequately blocked in the small format device from being absorbed by the detector. The performance measurement of the small format device including the luminescence will be presented in this section and the last section will discuss the design modifications implemented in the 128x128 device to reduce the luminescence for zodiacal background observations.

Good focal plane response uniformity has been achieved as shown in Figure 13. The histogram shows that the central 36 elements have a 6 percent, 1 sigma, response variation. This uniformity is typical when the anomalous edge element response is excluded.

The typical read noise for the small format device is shown in Figure 14 as a function of integration time. The upper curve was obtained by a device measured at the University of Hawaii. At short exposure times less than 10 seconds the read noise is about 150 electrons and at longer integration times the noise was limited by the shot noise of the luminescent current. Better measurement with a read noise less than 100 electrons have been obtained at Honeywell as shown in the figure. A Honeywell built low noise clock driver for the input reset clock, which couples directly into the detector signal, has allowed the improved measurement to be achieved. These measurements were obtained on hybrid devices using the multiplexers from the second fabrication lot which exhibited significantly higher 1/f noise which becomes the dominant source of read noise. If focal planes could have been fabricated on the initial multiplexer lot the read noise would be considerably lower as shown by the dotted line in the figure. The contributions due to the preamplifiers 1/f noise and Johnson noise is about 20 and 40 rms electrons, respectively, for a total read noise of 45 rms electrons.

The low detector dark current was not measurable on the small format device because of the stray detector current resulting from the luminescent photons generated by the active silicon devices within the multiplexer. The wavelength of these luminescent photons is near

the bandgap of silicon and are readily absorbed by the SWIR detectors. Their intensity has been shown to be a function of the current passing through the active silicon devices. Figure 15 demonstrates the extent to which the luminescence can be reduced by lowering the operating power of the multiplexer. The three 8x8 two dimensional maps illustrate relative intensity of the luminescence observed by each detector. Note that the left most map illustrates a very bright source in the lower corner which is due to the high power output buffer being continually on. By switching this buffer off except during readout times the bright source is eliminated. Although less than 100 electrons/second have been measured on the small feasibility device the typical luminescent current under optimal operating conditions is typically about 200 electrons/second. In order for this focal plane approach to be useful down to the zodiacal background levels, the luminescent photons must be blocked to prevent the absorption by the detectors. An effective approach to block these photons is presented in the next section.

6.0 IMPROVEMENT TO THE 128X128 DESIGN

The performance evaluation of the small format device has been most valuable in optimizing our approach in the design of the 128x128 focal plane. Scaling down to the smaller 2 mil square detector parameters leads directly to improved performance. The read noise for the device is directly related to the combined detector, input stray, and feedback capacitances which have been reduced 60 percent. Thus with typical 1/f noise for the input preamplifiers of 1 to 2 $\mu\text{v}/\sqrt{\text{Hz}}$ the read noise can be expected to be between 25 and 30 rms electrons. The feedback capacitor has been reduced to attain an input signal gain of 10. This minor modification allows the entire input circuit to readily fit within a 2 mil square cell, with the most critical element, the differential amplifier, retaining the identical configuration as used on the small format multiplexer. The usable charge capacity is 1.6×10^5 electrons over the 1 volt linear region of the amplifier yielding a dynamic range of 74 dB.

The approach to reduce the luminescent current is several fold. Scaling to the 128x128 device reduces the luminescent sources per detector element by a factor of two. The metal interconnect coverage within the unit cell has been increased from 66 percent in the small format device to 83 percent in the 128x128 design with special attention to cover active regions. Peripheral luminescent sources such as the output buffer and shift registers have been moved as far from the active detectors as possible, and generally masked with a reflecting layer. And because the luminescence is presumed to be emitted isotropically with low reabsorption within the silicon, an absorber placed on the backside of the silicon multiplexer substrate will prevent the photons from being reflected back up to the detectors. With these design approaches the resultant luminescent current is expected to be less than 10 electrons/second. Additional improvements are possible with an absorbing layer placed between the multiplexer and the detector.

In summary, the benefits of the charge integrating differential input preamplifier have been demonstrated on the small format focal plane. The 128x128 design is only a small evolutionary step and incorporates an effective approach to minimize the luminescent current present with this approach. This design provides a very linear output for accurate radiometric measurement placing minimum requirement on system calibration. The input preamplifiers maintain near zero bias across the entire array, minimizing detector dark current and 1/f noise, and to achieve optimal detector uniformity. Signal gain of order 10 eases off focal plane electronic low noise considerations. The non-destructive array reads offered by this approach support signal processing functions to achieve low noise performance and immunity to spurious noise events.

7.0 REFERENCES

1. N. M. Hartle et al., IRIS Detector Specialty Group Meeting, Moffet Field, CA, August 1986.
2. D. L. DePoy et al., Proceedings of the Second Infrared Detector Technology Workshop, Moffet Field, CA, August 13-14, 1985, p.16-1
3. N. Hartle et al., Proceedings of the Workshop on Ground-based Astronomical Observations with Infrared Detectors, Hilo, HA, March 24-26, 1987, p. 21
4. J. A. Stobie et al., IRIS Detector Specialty Group Meeting, Seattle, WA, August 11-13, 1987

*This work has been supported in part by the Jet Propulsion Laboratory, Pasadena CA, under Contract #958095, D. Ritchie technical monitor, and Dr. D. Hall principle investigator from the University of Hawaii.

Table 1. Performance Summary of the Small Format Device and Expected Performance for the 128 x 128 FPA.

	<u>Small Format Device Meas.</u>	<u>128x128 FPA Expectation</u>
Operating Temp (K)	80	80
Detector	LPE HCT	LPE HCT
size (mil square)	4	2
Cutoff Wavelength (um)	2.5	2.5
Quantum Efficiency (%)	70	>70 w/AR
Impedance ($10^{16} \Omega$)	0.4 - 4.0	0.7 - 11.0
Capacitance (pf)	0.4	0.2
Crosstalk (%)	< 2	< 3
Fill Factor (%)	75	80
Dark Current (e/s)	-	< 10
Focal Plane	CIDA x-y	CIDA x-y
Read Noise (rms e)	100 [*]	< 30
Dark Current (e/s)	-	< 10
Luminescence Current (e/s)	100-500	< 10 [†]
Charge Capacity (e)	3.2×10^5	1.6×10^5
Power Dissipation (mW)	0.3	< 80

* Limited by atypically high noise CMOS process run

†Luminescence Reduction Layers included

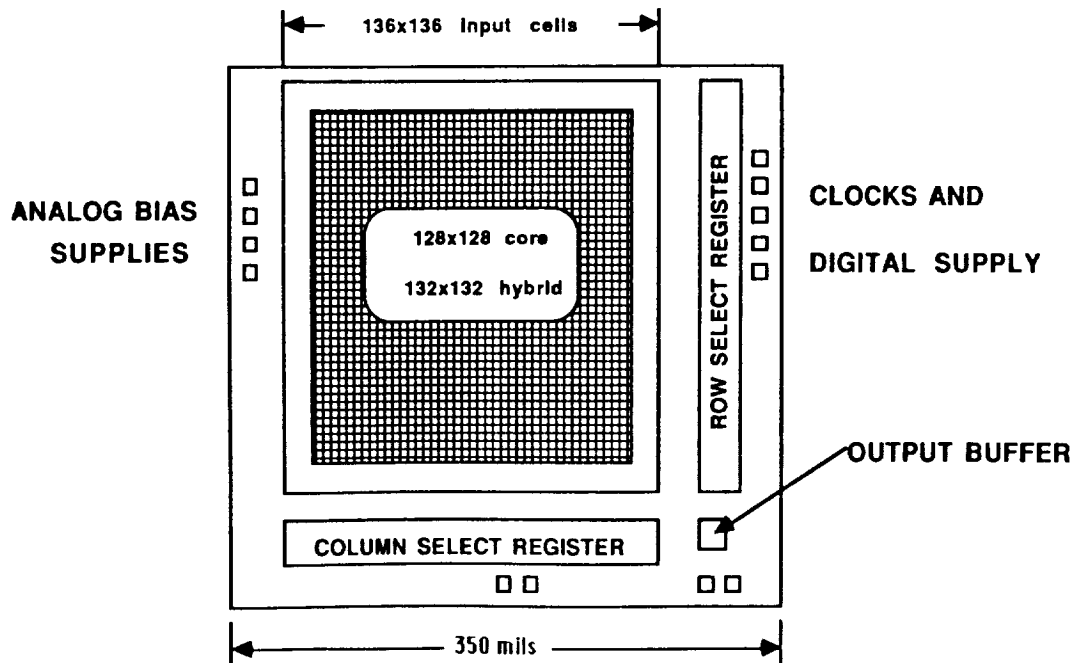


Figure 1. The 128 x 128 SWIR Focal Plane is a Hybrid Structure Consisting of HgCdTe Detectors and a Silicon CMOS Readout Device.

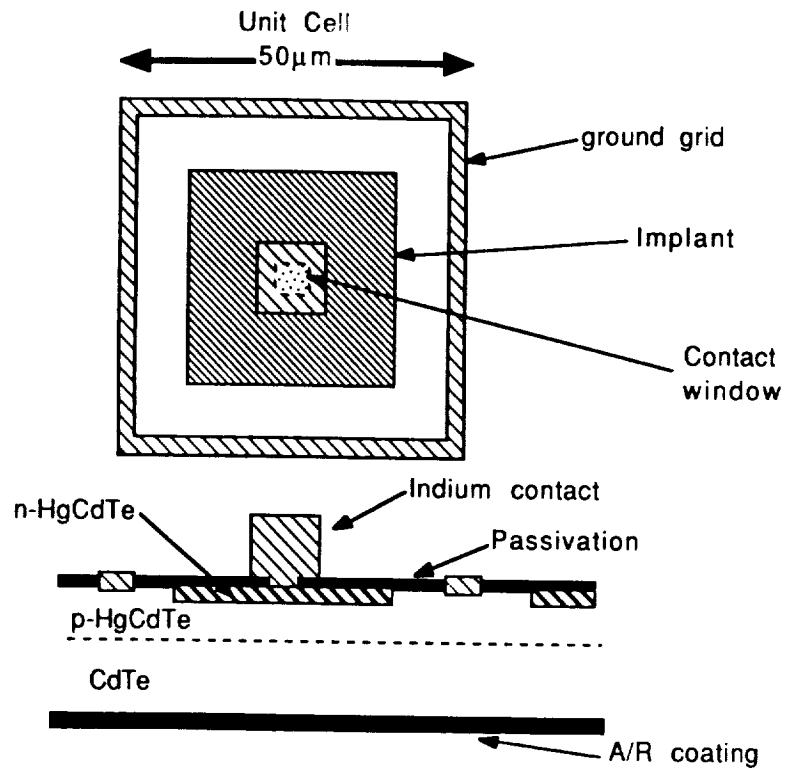


Figure 2. The LPE Grown HgCdTe Detectors are Fabricated Using a Highly Produccible Planar Design Approach.

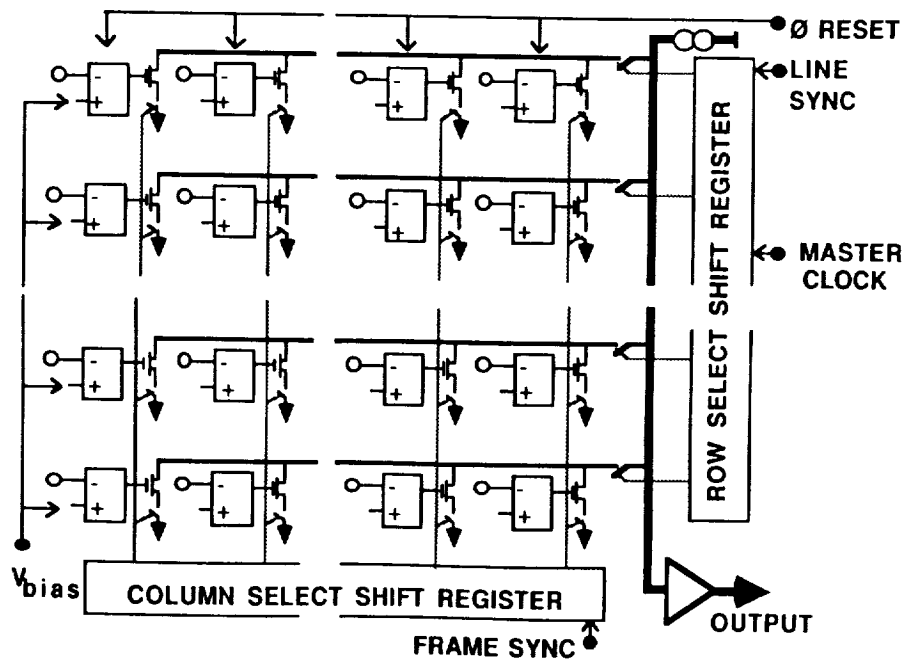
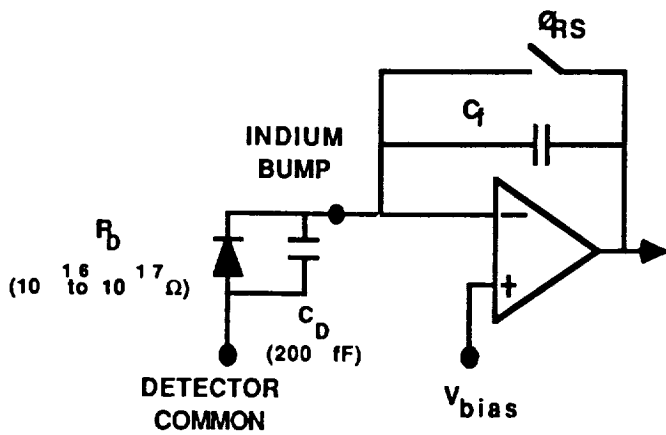


Figure 3. The Readout Multiplexer Uses a Proven Low Noise Non-Destructive x-y Readout Design.



BENEFITS

- 2 Mil Square Cell
- Maintains Near Zero Bias <3 mv, 1 sigma
- Read Noise Contribution to FPA <30 rms e
- Transimpedance Gain 6 uv/e
- Dark Current < 2 e/s
- Excellent Gain Uniformity 1 sigma variation <1 %
- Linearity Deviation <2 %
- Charge Capacity $1.6 \times 10^5 e$

Figure 4. The Charge Integration Differential Amplifier (CIDA) is an Excellent Preamplifier for Low Background SWIR PV Detectors.

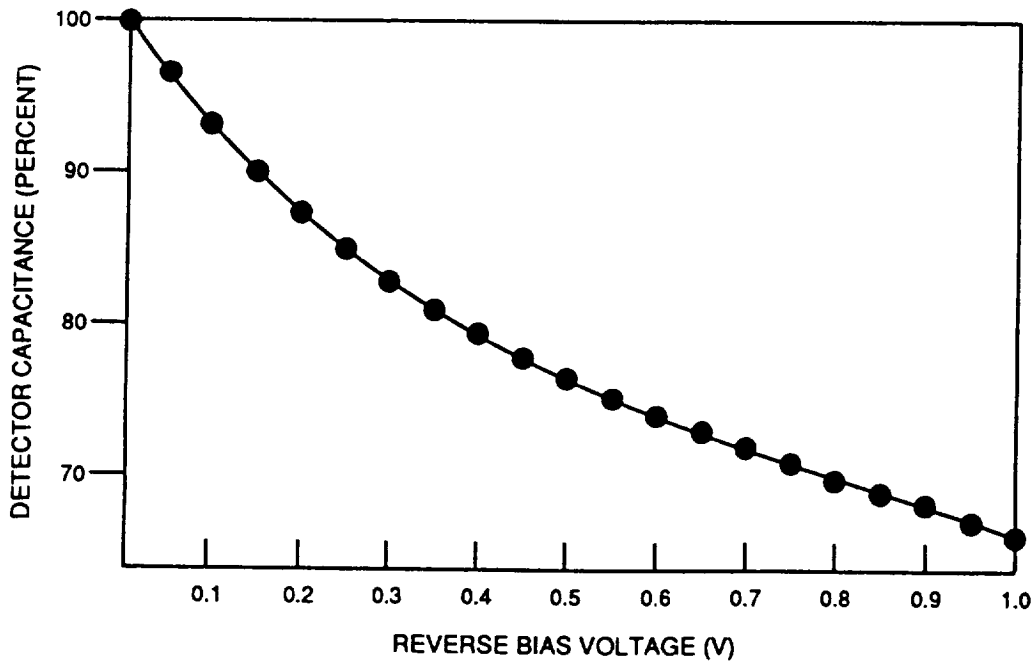


Figure 5. SWIR HgCdTe Detector C-V Characteristics is Clearly Not Constant With Bias Voltage.

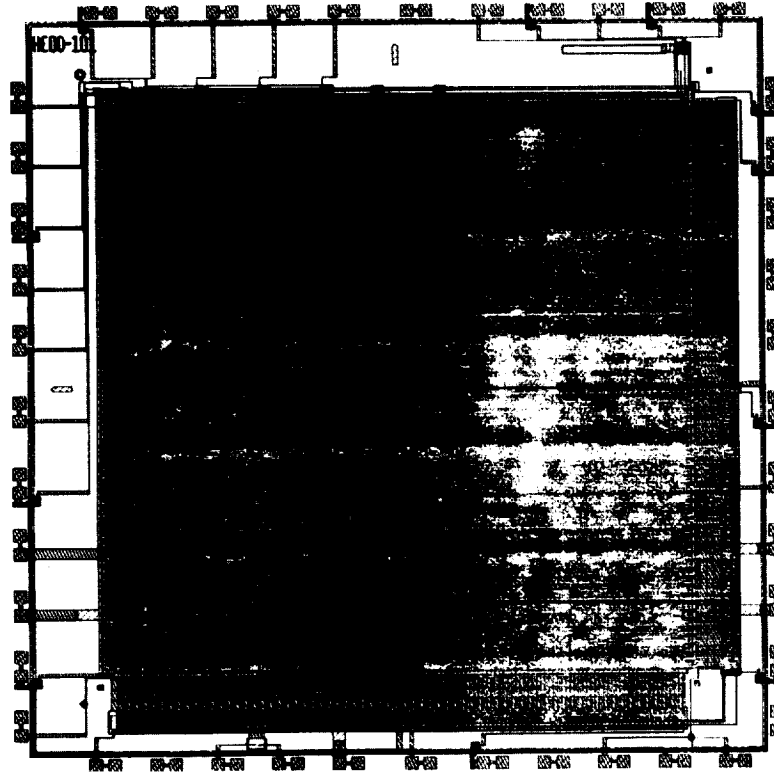


Figure 6. The 128 x 128 SWIR Multiplexer is Fabricated Using a Standard Production 1.2 Micron CMOS Process.

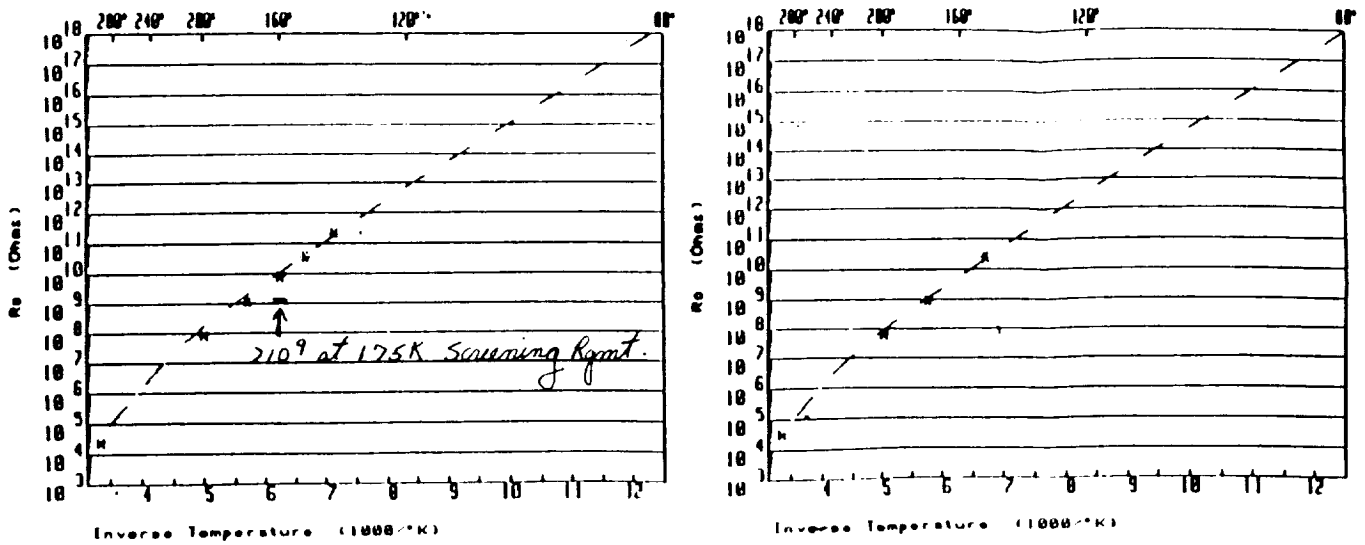


Figure 7. Routine Screening Tests for SWIR Detector are Limited to Impedance Less Than 10^{12} ohms Without Exotic Low Capacitance Coupling Schemes.

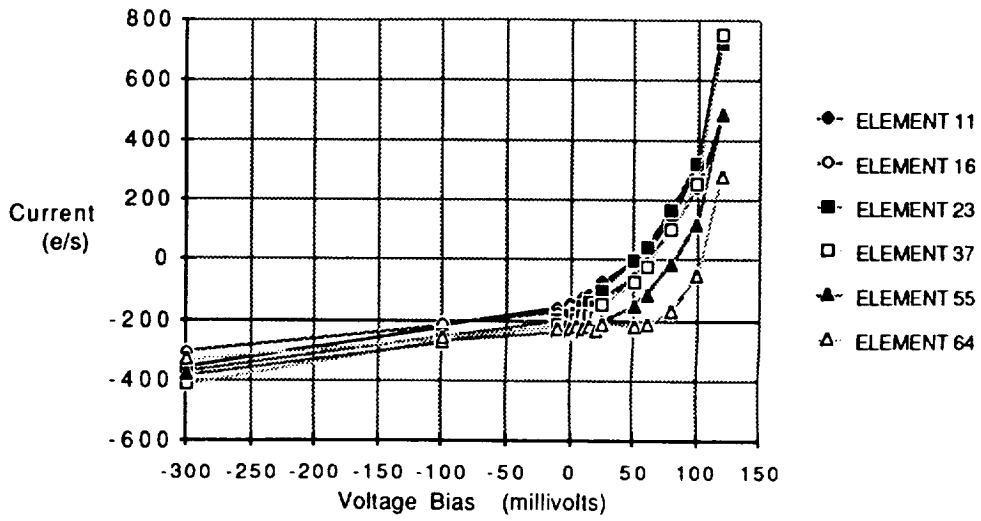


Figure 8. The CIDA Multiplexer is Ideally Suited to Measure the Detectors I-V Characteristics at 80K With dynamic Impedance in Excess of 10^{18} ohms.

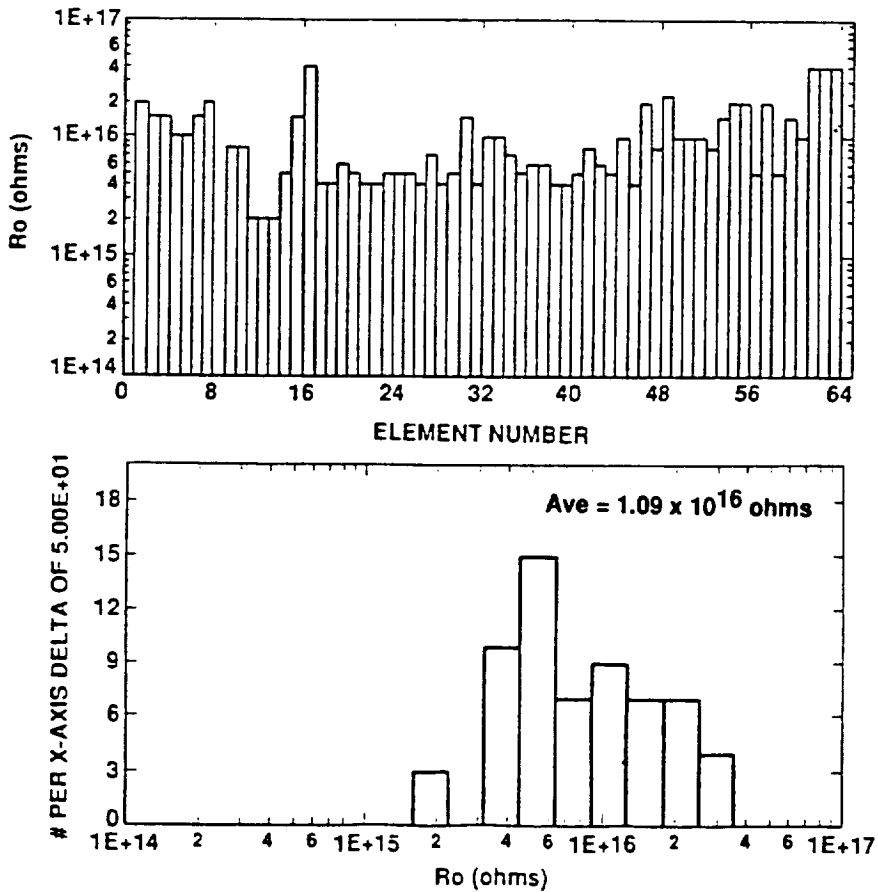


Figure 9. The Uniformity of the Detectors Zero Bias Impedance is Good at 80K.

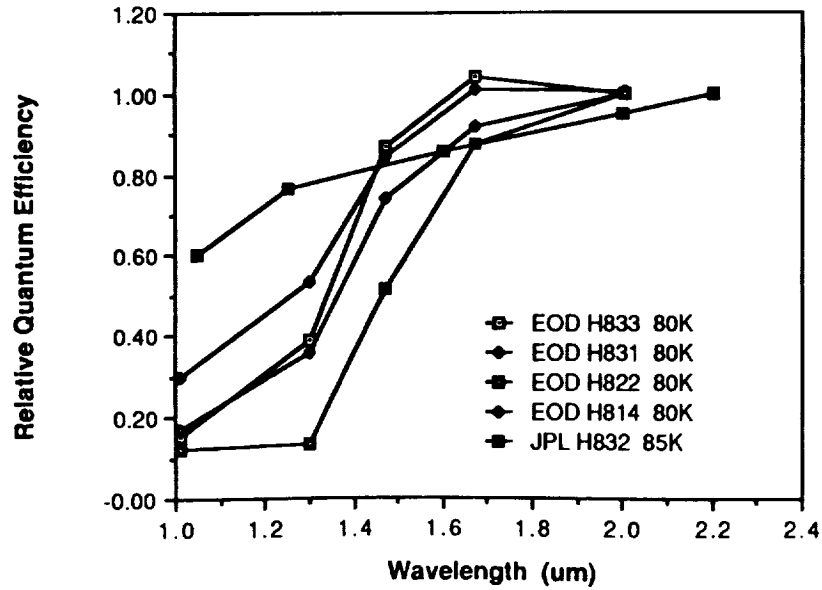


Figure 10. HgCdTe Detectors Achieve 70 Percent Quantum Efficiency Above 1.6 micron at 80K. (No AR Coating)

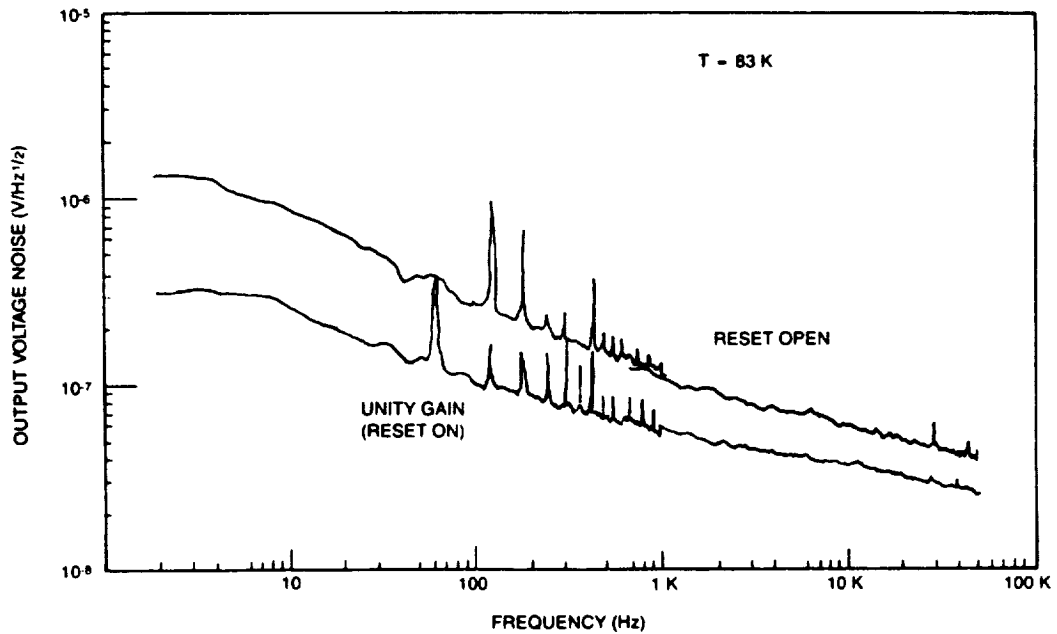


Figure 11. The Initial Lot of Multiplexers Demonstrated the CIDA Input 1/f Noise is Sufficiently Low to Achieve a Read Noise of 20 rms electrons.

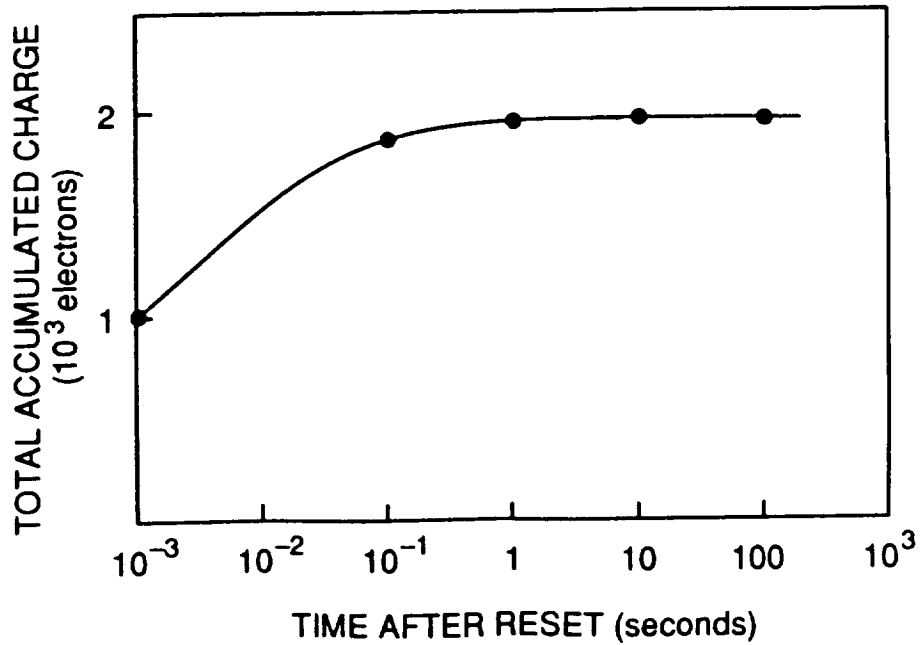


Figure 12. For Optimum Performance a Short Settling Time (0.1 to 1 sec) is Required Following the Reset Operation to let the Circuit Return to Equilibrium.

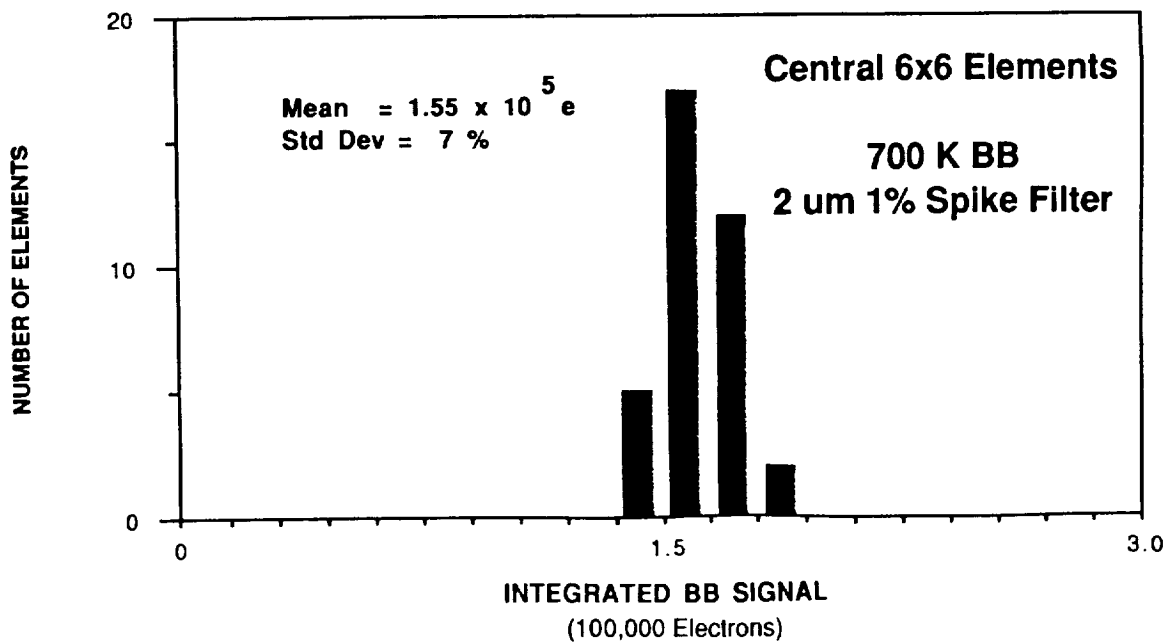


Figure 13. Excellent Response Uniformity is Obtained with a 7 Percent Standard Deviation.

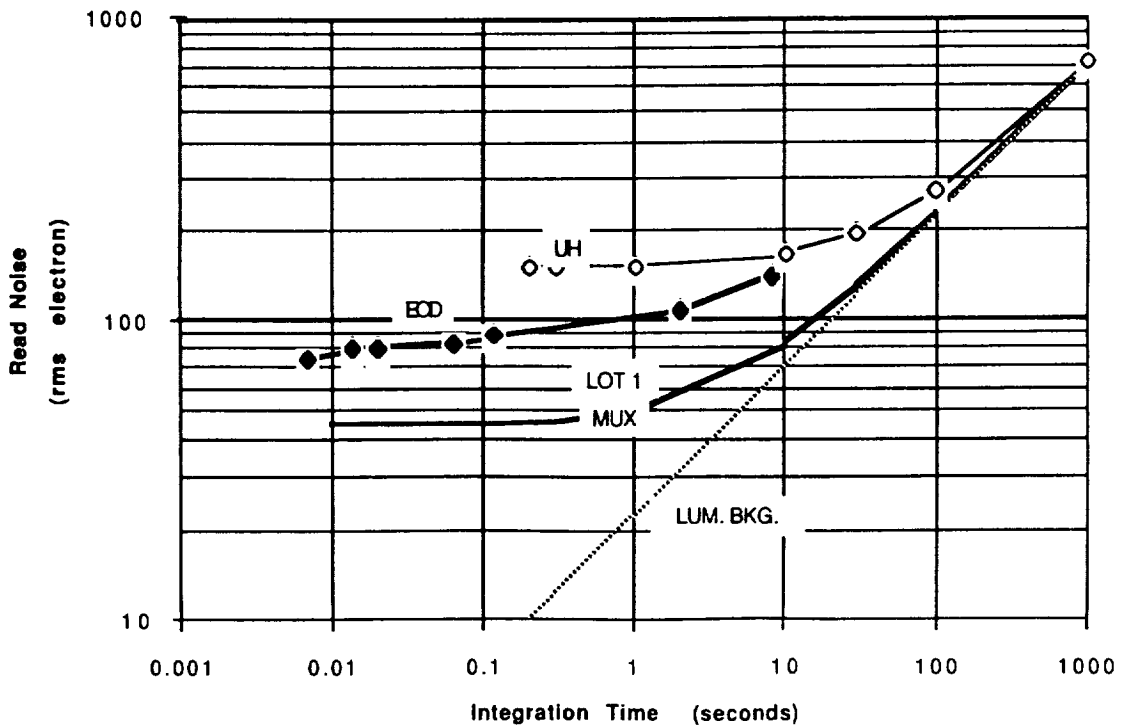


Figure 14. The Measured Read Noise Agrees Well With Theory for Lot 2 Multiplexers with Unusually High 1/f Noise.

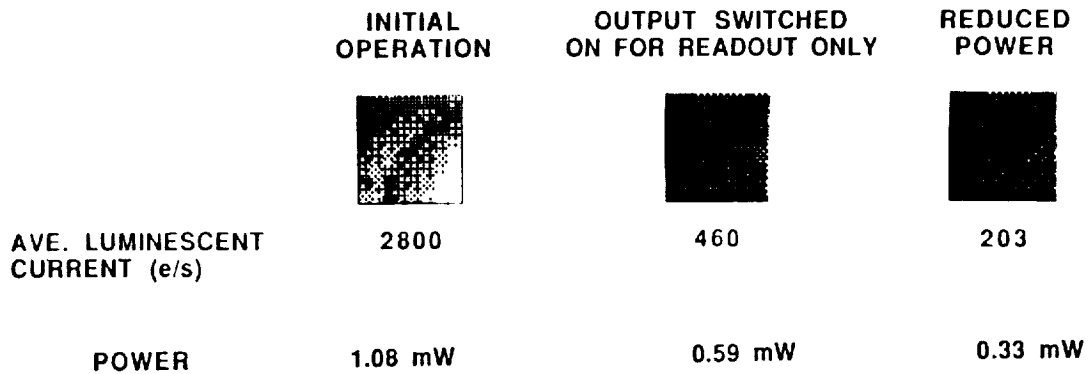


Figure 15. Lowering the Active Power Dissipation on the FPA Substantially Reduces the Luminescence Current.